https://doi.org/10.5194/egusphere-2026-1577
Preprint. Discussion started: 11 May 2026

Molecular dynamics study on the liquid-liquid contact angle in liquid-liquid phase separated aerosols

Chao Zhang[1, 2, 3], Leyi Liu[1], Shaopeng Li[1], Haoyang Lin[1], Yang Yang[1, 2*], Nan Ma[4], Yueshe Wang[5], Alfred Wiedensohler[6]

[1] School of Energy and Power Engineering, University of Shanghai for Science and Technology, Shanghai 200093, China

[2] Shanghai Key Laboratory of Multiphase Flow and Heat Transfer in Power Engineering, University of Shanghai for Science and Technology, Shanghai 200093, China

[3] State Key Laboratory of Atmospheric Environment and Extreme Meteorology, Institute of Atmospheric Physics, Chinese Academy of Sciences, Beijing 100029, China

[4] Institute for Environmental and Climate Research, College of Environment and Climate, Jinan University, Guangzhou, Guangdong 511443, China

[5] State Key Laboratory of Multiphase Flow in Power Engineering, Xi'an Jiaotong University, Xi'an 710049, China

[6] Leibniz Institute for Tropospheric Research, 04318, Leipzig, Germany

Correspondence to: yangyang@usst.edu.cn

https://doi.org/10.5194/egusphere-2026-1577
Preprint. Discussion started: 11 May 2026

Abstract

The contact angle is a key parameter in describing the morphology of liquid-liquid phase separated (LLPS) aerosols. However, existing experimental methods are unable to precisely measure the contact angle at the nanoscale. Here, molecular dynamics (MD) simulations based on Martini force field and OPLS-UA force field are conducted to reveal the effects of temperature, water content, inorganic salt (NaCl) content and surfactant (suberic acid) content on the liquid-liquid contact angle in water-dodecane LLPS aerosols, and the applicability of classical Young's equation is analyzed. MD simulations show that the contact angle is positively correlated with temperature and water content but is negatively correlated with NaCl content and suberic acid content. The Martini force field generally results in larger contact angles and stronger influence of NaCl than the OPLS-UA force field. Interfacial tensions of gas-water and water-dodecane calculated based on the OPLS-UA force field are closer to the experimental results. At the nanoscale, the contact angle calculated by Young's equation always deviates significantly from MD simulations, necessitating the inclusion of line tension. Furthermore, reliable line tensions for different systems have been obtained and fitted with a quartic polynomial function.

Keywords: Aerosol, liquid-liquid phase separated, contact angle, molecular dynamics

1. Introduction

Atmospheric aerosols have great impact on the Earth's climate directly by absorbing, reflecting and scattering solar radiation and indirectly by acting as cloud condensation and ice nuclei influencing formation of clouds and precipitation (Tang

https://doi.org/10.5194/egusphere-2026-1577
Preprint. Discussion started: 11 May 2026

and Munkelwitz, 1994; Yu et al., 2006; You et al., 2012). Effects of aerosols on climate are influenced by the aerosol size, physical state, chemical composition and morphology (Martin, 2000). Therefore, understanding the interrelation between chemical composition and aerosol phase is critical to global air quality and climate models and related future climate projections.

Atmospheric aerosols are found to be composed of several types of inorganic salts and thousands of organic compounds (Noziere et al., 2014). Liquid-liquid phase separation (LLPS) has been observed in numerous laboratory-generated and atmospheric aerosols. In the LLPS aerosols, depending on the solubility of the organic compound, an aqueous salt-rich phase and a potentially aqueous organic-rich phase are in contact with each other (Song et al., 2012; Schmedding and Zuend, 2025). There are two main morphologies of LLPS aerosols: core-shell (total wetting of one phase by the other) and partial wetting (asymmetric structures, with one phase partially engulfed by the other) (Qiu and Molinero, 2015; Freedman, 2017). The morphology of LLPS aerosols has a significant impact on their aging through hygroscopic growth and heterogeneous chemistry reaction.

Numerous studies have focused on the influencing factors, particle structure, and inter-phase component distribution of LLPS aerosols. In terms of experimental studies, the experimental methods for the LLPS of aerosol particles can be divided into substrate method and single particle suspension method. Instruments used in the substrate method generally include the optical microscope (Huang et al., 2021; Song et al., 2012), transmission electron microscopy (TEM) (Veghte et al., 2013) and scanning transmission X-ray microscopy/near edge X-ray absorption fine structure (STXM/NEXAFS) (O'brien et al., 2015). In order to reduce the influence of the substrate on the droplet structure, hydrophobically coated substrates are used. In the

https://doi.org/10.5194/egusphere-2026-1577
Preprint. Discussion started: 11 May 2026

single particle suspension method, particle is suspended under the action of electric field force or single beam gradient force optical trap (Ingram et al., 2021; Davies, 2019). Raman spectroscopy is always coupled to these techniques to present information on morphology and composition. Based on the above methods, some studies have investigated the phase structure of various organic-inorganic mixed aerosol particles under different relative humidities (Zuend et al., 2008), and results shows that the ratio of O atoms to C atoms (O:C ratio) in organic matter can be used as a key parameter to determine the occurrence of LLPS and the phase separation relative humidity (SRH). When mixed with ammonium sulfate, organic compounds with O:C < 0.56 undergo phase separation, while compounds with O:C ≥ 0.8 lead to homogeneous phase. Additionally, at 0.56 < O:C < 0.8, whether particles undergo LLPS depends on the type of organic functional groups.

In terms of theoretical research, LLPS is mainly driven by the non-ideality in the droplet of solution, and it can occur by nucleation, growth, and spinodal decomposition (Papon et al., 2006). Based on the thermodynamic equilibrium principle and the AIOMFAC (Aerosol Inorganic-Organic Mixtures Functional groups Activity Coefficients), Zuend et al. (2010) proposed the LLE-AIOMFAC to describe the inter phase component distribution inside the LLPS aerosols. LLE-AIOMFAC model has been applied in the descriptions of cloud condensation nuclei (CCN) activation and the unsteady hygroscopic growth process of LLPS aerosols (Ovadnevaite et al., 2017; Huang et al., 2021; Shiraiwa et al., 2013), which are crucial in large-scale climate models. Recently, LLE-AIOMFAC model has been improved to predict the LLPS inter phase component distribution in ultrafine particles by taking into account the size-dependent surface and interfacial tension effects (Schmedding and Zuend, 2025).

The elucidation of the internal structure of LLPS aerosols is important and

https://doi.org/10.5194/egusphere-2026-1577
Preprint. Discussion started: 11 May 2026

challenging, especially for nanoscopic aerosols. The contact angle between the two phases can be used to quantify the extent of wetting in the LLPS aerosols. The two limits are $\theta = 180°$ corresponding to nonwetting and $\theta = 0°$ to core-shell. In the study of fluid wetting on a solid surface, the Young's equation (Young, 1805), which predicts the contact angle using the interfacial tension of solid-liquid, solid-vapor and liquid-vapor, is the widely accepted wetting model at the macroscale. However, the three-phase line tension should be included in the Young's equation to calculate the contact angle in the surface nanodroplet (Jabbarzadeh, 2024). In the LLPS aerosols, Qiu and Molinero (2015) has demonstrated that for particles of diameter larger than ~100 nm the contact angle can be calculated by an expression that is identical to Young's equation, while for the ultrafine aerosols the contact angle depends also on the line tension between the two liquids and the vapor. Moreover, molecular dynamics (MD) simulations of nonane-water droplets were used to validate the thermodynamic predictions. In order to better predict the morphology of LLPS particles, further research on the contact angle is necessary.

In this study, MD simulation method is adopted to reveal the effects of temperature, water content, inorganic salt (NaCl) concentration and surfactant (suberic acid) concentration on the contact angle in the dodecane-water LLPS aerosols. Dodecane, which comes from the incomplete combustion or volatilization of fuel is used as a proxy for insoluble organic substances due to its abundant interfacial tension data in literatures (Schmidt et al., 1966; Sayed et al., 2019).

2. Computation details

2.1 MD simulations

The simulated objects included binary and ternary droplets. The binary droplets were consisted of 2000 dodecane molecules and different numbers of water molecules

https://doi.org/10.5194/egusphere-2026-1577
Preprint. Discussion started: 11 May 2026

(8000, 12000, 16000, 20000, 32000), while the ternary droplets contain 2000 dodecane molecules, 8000 water molecules and different amounts of NaCl (50, 100, 150, 200, 600, 800). The Martini coarse-grained (CG) force field (Marrink et al., 2007) and the united-atom force field (OPLS-UA) (Jorgensen et al., 1984) were employed to describe the interatomic interactions in the simulation systems, respectively. Both force fields are coarse-grained, which can effectively reduce computational costs and have been widely applied to quantify microscopic properties, including contact angles and interfacial tensions (gas-liquid, liquid-liquid) (Qiu and Molinero, 2015; Sergi et al., 2012).The size of the simulation box was 300 Å, and periodic boundary conditions were adopted. Details of the MD simulations are presented in the Supplement.

2.2 Contact angle

Fig. 1 shows a schematic diagram of LLPS droplets. The liquid-liquid contact angle (α) in the figure was calculated by

$$\alpha = \cos^{-1}\left(r_w^2 + r_o^2 - d^2\right) / \left(2 r_w r_o\right) \quad (1)$$

where r_w is the fitted radius of water molecule clusters, r_o is the fitted radius of dodecane molecule clusters, and d is the distance between the two centers of the spheres.

The acquisition of the radius of water molecule clusters and the radius of dodecane molecule clusters in the droplet were based on the accurate acquisition of the droplet contour. A coordinate system (r, z) was established with the centroid of the organic molecule cluster as the origin and d as the z-axis (Do Hong et al., 2009). The simulation system was divided into multiple cylindrical bins with same height (Δz = 2.5 Å) and same volume. Boundaries of radial bins are located at $d_i = \sqrt{i \cdot \delta A / \pi}$ with $i = 1\cdots\cdots$,

https://doi.org/10.5194/egusphere-2026-1577
Preprint. Discussion started: 11 May 2026

with a base area per bin of $\delta A = 380$ Å^2. The density distribution $\rho(r, z)$ of the entire droplet was obtained by calculating the number density of molecules in each cylindrical bin. The point with the minimum $\rho(r, z)$ in the gas-liquid droplet was selected as the gas-liquid interface. The droplet contour was obtained by fitting these interface points into a circle using the least square method.

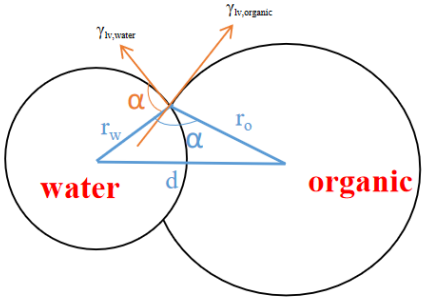

Fig. 1. Schematic diagram of the LLPS droplet

2.3 The interfacial tension

The interfacial tensions of the horizontal gas-liquid (pure water $\gamma_{g\text{-}w}$, pure dodecane $\gamma_{g\text{-}d}$) and liquid-liquid (water-dodecane $\gamma_{w\text{-}d}$) interfaces can be calculated by the following formulas:

$$\gamma = \frac{L_z}{2}\left\langle P_{zz} - \frac{1}{2}\left(P_{xx} + P_{yy}\right)\right\rangle \quad (2)$$

where P_{zz}, P_{xx}, and P_{yy} are the pressure tensors perpendicular to and tangential to the xy plane, respectively. L_z is the length of the simulation box in the z direction, perpendicular to the gas-liquid interface formed along the xy plane. Due to the existence of two interfaces, there is a factor of 1/2. The angle brackets indicate the average value taken over multiple time points. The simulation systems used to calculate $\gamma_{g\text{-}w}$ and $\gamma_{g\text{-}d}$ contain 2000 water molecules and 500 dodecane molecules, respectively, while the

https://doi.org/10.5194/egusphere-2026-1577
Preprint. Discussion started: 11 May 2026

system used to calculate $\gamma_{w\text{-}d}$ contains 500 dodecane molecules and 4000 water molecules. Each simulation system contains two equivalent alkane/gas, water/gas, and alkane/water interfaces, all of which are parallel to the *xy* plane. Additionally, for the surface tension of SPC/E water, to achieve results more consistent with experiments, the calculated pure water surface tension was corrected using the tail correction term (γ_d). For this purpose, the number density of the liquid along the z-axis was fitted to a hyperbolic tangent function.

$$\rho(z) = \frac{1}{2}(\rho_l + \rho_v) - \frac{1}{2}(\rho_l - \rho_v)\tanh\left(\frac{z - z_0}{\xi}\right) \tag{3}$$

where ρ_l and ρ_v represent the densities of the liquid and vapor phases, respectively. Then, the tail correction term (γ_d) is calculated according to the method of Blokhuis et al. (1995).

$$\begin{aligned}\gamma_d &= 12\pi\varepsilon\sigma^6(\rho_l - \rho_v)^2\int_0^1 ds\int_{r_c}^{\infty} dr\left(3s^3 - s\right)r^{-3}\coth\left(\frac{rs}{\xi}\right)\\ &= 12\pi\varepsilon\sigma^6(\rho_l - \rho_v)^2\int_0^1 ds\int_0^{\frac{r_c}{s}} dr'\left(3s^3 - s\right)r'\coth\left(\frac{s}{r'\xi}\right)\end{aligned} \tag{4}$$

To ensure the reliability of the simulation results, we conducted the simulation three times for the same system. Additionally, since the contact angle of two nanoscale droplets was investigated, the influence of curvature on surface tension should be included. Tolman (1949) proposed the relationship between surface tension and radius for equimolar dividing surface (*Re*), which is shown below:

$$\gamma'_{g-w(d)} = \frac{\gamma_{g-w(d)}}{\left(1 + \frac{2\delta}{Re}\right)} \tag{5}$$

where $\gamma'_{g-w(d)}$ represents the surface tension of a droplet with *Re*, and δ is the Tolman length. In formula (5), the sign of the Tolman length is positive for a droplet (convex

https://doi.org/10.5194/egusphere-2026-1577
Preprint. Discussion started: 11 May 2026

interface) and negative for a bubble (concave interface). Therefore, when the radius of curvature *Re* is comparable to the Tolman length δ, the surface tension of the droplet decreases as the droplet size decreases. δ of water is approximately 0.048 nm (Leong and Wang, 2018). Meanwhile, for short-chain alkanes such as pentane and dodecane, the recommended δ is 0.035 nm (Rehner et al., 2019). For NaCl droplets, the recommended δ is 0.1 nm (Bahadur and Russell, 2008). *Re* is obtained through the density profile fitting (Equation (3)).

3. Results and discussions

3.1 Contact angle of binary water-dodecane LLPS droplets

For LLPS droplets composed of water and dodecane, we investigated the effects of temperature and the water content on the binary contact angle. The snapshots of the equilibrium droplets based on the Martini force field MD simulations are shown in Fig. 2. Results based on the OPLS-UA force field MD simulations present the similar result and are presented in Fig. S2 (Supplement).

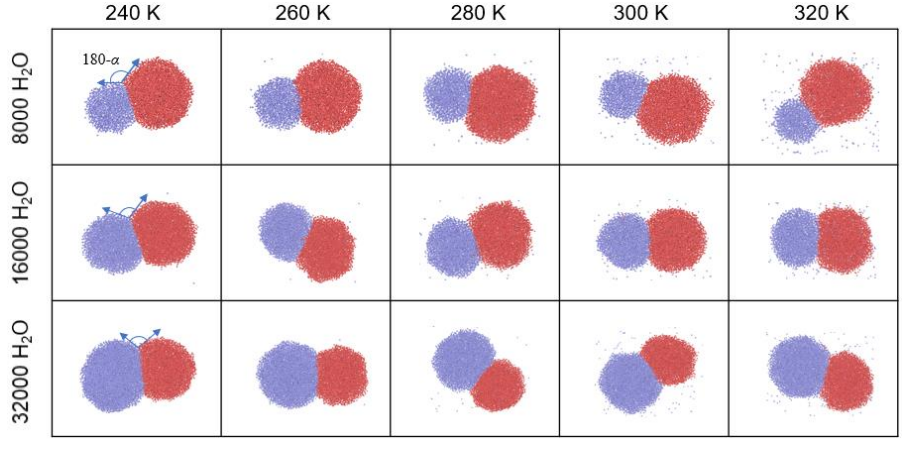

Fig. 2. Snapshots of water-dodecane droplets under different temperatures and water contents

https://doi.org/10.5194/egusphere-2026-1577
Preprint. Discussion started: 11 May 2026

(MD simulations with Martini force field）, dodecane and water molecules are represented by red and blue balls, respectively

As shown in Fig. 2, at the equilibrium state all water-dodecane binary droplets exhibit the "Russian doll" type LLPS structure, so-called because spherical nonane lens partially wets a spherical water droplet, and the droplet shape is similar to the popular children's toy. This result is consistent with the reported water-nonane binary droplet equilibrium structure in the literature (Obeidat et al., 2015; Qiu and Molinero, 2015), and this behavior is primarily due to the immiscibility between water and alkanes. Under the same temperature condition, as the water content increases, the size of the water clusters increases, and the liquid-liquid contact angle shows a tendency to increase. However, the influence of temperature on the liquid-liquid contact angle cannot be clearly determined from Fig. 2. Based on the qualitative description, we further studied the mechanisms of temperature and water content on the liquid-liquid contact angle of the water-dodecane binary droplet, using the contact angle calculation method described in Section 2.2. Corresponding results are shown in Fig. 3, in which outcomes based on both the Martini force field and the OPLS-UA force field are included.

https://doi.org/10.5194/egusphere-2026-1577
Preprint. Discussion started: 11 May 2026

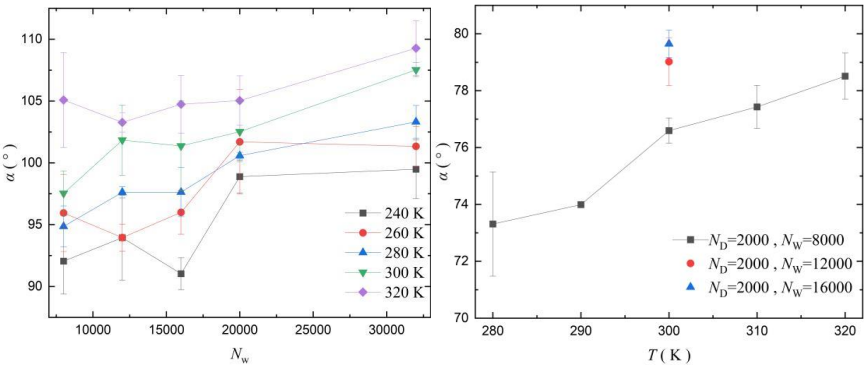

(a) (b)

Fig. 3. Contact angles of water-dodecane droplets under different temperature and water content conditions. (a) Results of Martini force field, and (b) results of OPLS-UA force field

As shown in Fig. 3(a), when the temperature is constant, the contact angle is positively correlated with the number of water molecules, which is consistent with the qualitative results obtained from Fig. 2. In addition, when the content of water molecules in the droplet is the same, the contact angle shows an increasing trend with the increase of temperature. This result is consistent with the variation of the contact angle between nonane and water with temperature in Obeidat et al. (2015). It can be seen from Fig. 3(b) that the contact angle obtained based on the OPLS-UA force field is positively correlated with both temperature and water molecule content, which is consistent with the result based on the Martini force field. The mechanism of temperature's effect on contact angle will be discussed in the Discussions section (Section 3.5), taking into account the results of changes in interfacial tension. However, under the same conditions, the contact angle values obtained based on the OPLS-UA force field is smaller than those of the Martini force field.

3.2 Contact angle of ternary water-dodecane-NaCl LLPS droplets

https://doi.org/10.5194/egusphere-2026-1577
Preprint. Discussion started: 11 May 2026

In this section, we investigated the effects of temperature and NaCl concentration on the liquid-liquid contact angle in ternary LLPS droplets composed of dodecane, water, and NaCl. It should be noted that NaCl is presented only in the water clusters. Fig. 4 presents simulation snapshots of water-dodecane-NaCl droplets under different NaCl contents and temperatures. The results based on both the Martini force field and the OPLS-UA force field are shown in the figure.

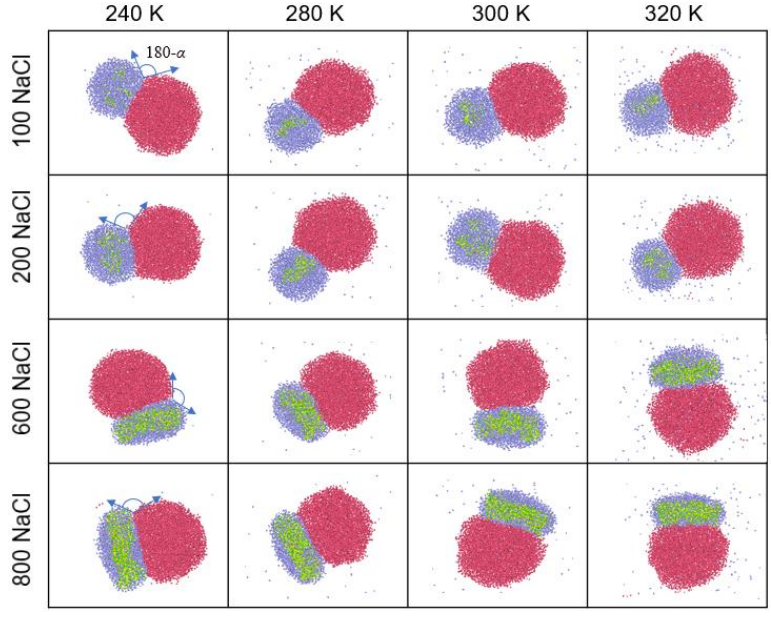

(a)

https://doi.org/10.5194/egusphere-2026-1577
Preprint. Discussion started: 11 May 2026

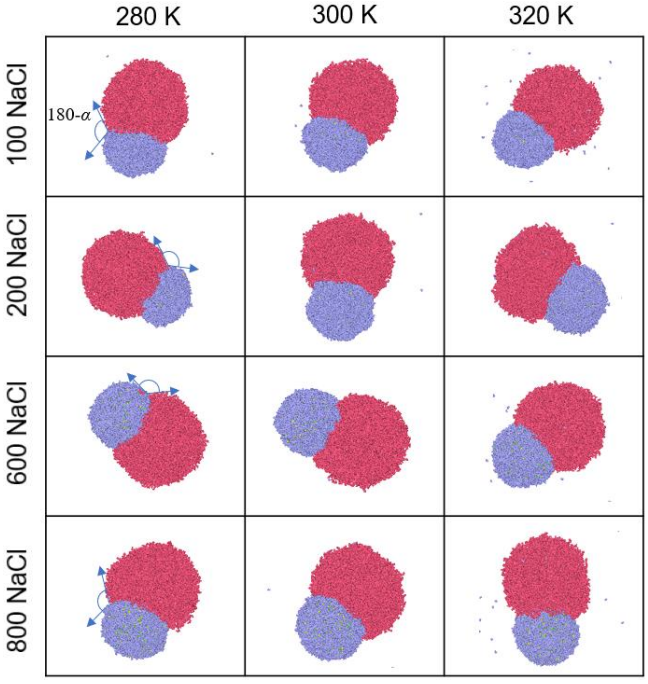

(b)

Fig. 4. Simulated snapshots of water-dodecane-NaCl droplets under conditions of different NaCl contents and temperatures ((a) Martini force field, (b) OPLS-UA force field). Dodecane, water, Na^+ and Cl^- are represented by red, blue, green and yellow balls, respectively

Based on the Martini force field, Fig. 4(a) shows that at the NaCl concentration of 100 and 200, the water-NaCl clusters and dodecane clusters in ternary droplets under all four temperature values (240-320 K) present approximately spherical shapes. However, when the NaCl content increases to 600, there is a noticeable increase in the degree of aggregation of NaCl at the center of the water molecule clusters, resulting in an elongated shape with water molecules enveloping the NaCl aggregates. Consequently, the overall water-NaCl cluster presents an ellipsoidal shape. Compared to spherical water and dodecane clusters, distance between the mass center of the

https://doi.org/10.5194/egusphere-2026-1577
Preprint. Discussion started: 11 May 2026

ellipsoidal water cluster and the dodecane cluster exhibit a significantly reduction, which results in a decrease in the liquid-liquid contact angle according to Equation (1).

When the OPLS-UA force field is employed (Fig. 4(b)), all water-NaCl clusters exhibit a spherical shape under various NaCl content and temperature conditions. The discrepancy in cluster structures arising from the two different force fields can be attributed to the following factors. In the Martini force field, four water molecules are represented by one bead, so the number of the water bead is one fourth of the OPLS-UA force field, which may thereby reduce the solubility capacity for NaCl. At larger NaCl concentration, the NaCl aggregate exert a dominant influence on the shape of the water-NaCl clusters.

In order to quantitatively describe the effect of NaCl concentration and temperature on the contact angle in ternary dodecane-water-NaCl droplets, Fig. 5 presents the liquid-liquid contact angle as a function of NaCl concentration at different temperatures using the Martini force field and the OPLS-UA force field.

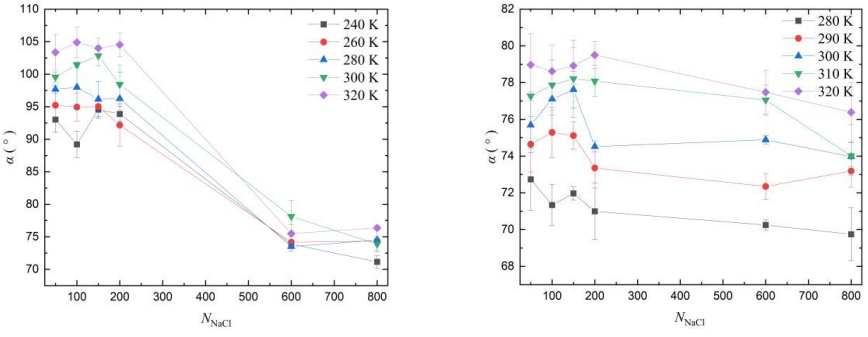

(a) (b)

Fig. 5. The liquid-liquid contact angle as a function of NaCl concentration at different temperatures in ternary water- dodecane-NaCl droplets ((a) the Martini force field, (b) the OPLS-

https://doi.org/10.5194/egusphere-2026-1577
Preprint. Discussion started: 11 May 2026

UA force field)

As shown in Fig. 5(a), when the NaCl content increases from 50 to 200, No substantial change in the contact angle is generally observed under isothermal conditions. However, when the NaCl content increases from 200 to 600 and 800, a notable decrease in the contact angle is observed under the same temperature conditions. This significant reduction in the contact angle corresponds to the phenomenon observed in Fig. 4, where the water-NaCl clusters transition from a spherical to an ellipsoidal shape. Furthermore, at a constant NaCl content, the contact angle in the ternary droplets increases with rising temperature. When molecular simulations are conducted using the OPLS-UA force field (Fig. 5(b)), the contact angle generally exhibits a negative correlation with NaCl content and a positive correlation with temperature, which is qualitatively consistent with the results based on the Martini force field. The negative correlation between contact angle and NaCl content will be elaborated in the Discussion section (Section 3.5), considering the changes in interfacial tensions. However, in contrast to the results obtained with the Martini force field, no significant decrease in the contact angle was observed when the NaCl content increased from 200 to 600. Additionally, under the same NaCl content and temperature conditions, the contact angle calculated using the Martini force field is approximately 2-20° smaller than that obtained using the OPLS-UA force field, and the difference is more pronounced at lower NaCl content.

3.3 Contact angle of ternary water-dodecane-suberic acid LLPS droplets

In this section, effects of temperature and NaCl concentration on the liquid-liquid

https://doi.org/10.5194/egusphere-2026-1577
Preprint. Discussion started: 11 May 2026

contact angle in ternary LLPS droplets composed of dodecane, water, and suberic acid ($C_8H_{14}O_4$) are investigated. Due to the absence of Martini force field parameters in suberic acid, only the OPLS-UA force field was employed. Simulation snapshots of water-dodecane-suberic acid droplets under different suberic acid number (50, 100, 150, 200) and temperature (280 K, 290 K, 300 K, 310 K, 320 K) conditions are shown in Fig. 6. To present the distribution of suberic acid, water and suberic acid are displayed separately at the temperature of 280 K.

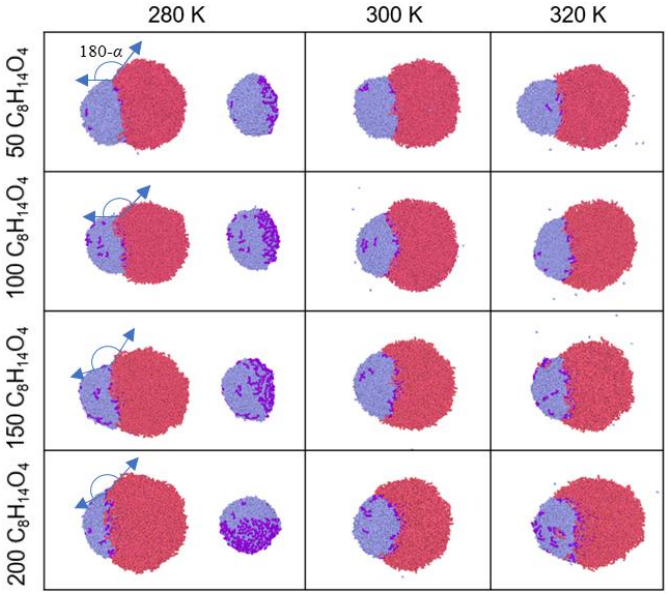

Fig. 6. Snapshots of water-dodecane-suberic acid ($C_8H_{14}O_4$) droplets under different temperatures and $C_8H_{14}O_4$ contents (MD simulations with OPLS-UA force field), and water and suberic acid in the particles are depicted at T = 280 K. Dodecane, water, and suberic acid are represented by red, blue and purple balls, respectively

As shown in Fig. 6, all water-dodecane-suberic acid ternary droplets exhibit the "Russian doll" type LLPS structure with two spherical contours, which is similar to the

https://doi.org/10.5194/egusphere-2026-1577
Preprint. Discussion started: 11 May 2026

binary water-dodecane droplets shown in Fig. 2. Most of the suberic acid molecules appear at the junction of hydrated dodecane, with a small portion distributed on the surface of water molecule hemisphere. This phenomenon is consistent with the molecular dynamics simulation results of malonic acid (-adipic acid)-eicosane-water droplet (Zhang et al., 2024) and cis-pinonic acid-*n*-triacontane-water droplet (Karadima et al., 2019). In Fig. 6, it is difficult to distinguish the effect of temperature on the contact angle, but the increasing suberic acid significantly increases the degree of encapsulation of water molecules by dodecane, which indicates an increasing contact angle.

In order to quantitatively describe the effect of suberic acid concentration and temperature on the contact angle in ternary dodecane-water-suberic acid droplets, the liquid-liquid contact angle as a function of temperature at different suberic acid contents are presented in Fig. 7.

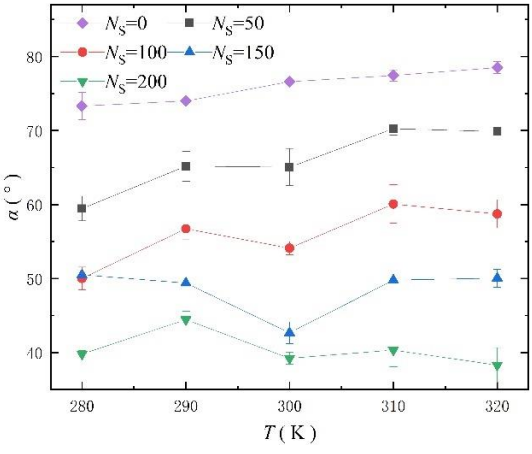

Fig. 7. The liquid-liquid contact angle as a function of temperature at different suberic acid contents in ternary water- dodecane-suberic acid droplets

https://doi.org/10.5194/egusphere-2026-1577
Preprint. Discussion started: 11 May 2026

As shown in Fig. 7, the liquid-liquid contact angle decreases obviously with the increase of suberic acid content at different temperatures. This phenomenon can be qualitatively explained by the appearance of suberic acid containing both hydrophilic and oleophilic groups at the interface between water and dodecane, which enhances the contact area between water and dodecane. A detailed explanation of the relationship between suberate concentration and contact angle is presented in the Discussion section (Section 3.5). Fig. 7 also illustrates that when the content of suberic acid is 50 and 100, the liquid-liquid contact angle increases with the increase of temperature, which is consistent with the result of binary dodecane-water system. However, when the number of suberic acid increase to 150 and 200, the absolute value of the slope of the relationship between temperature and contact angle decreases obviously, which demonstrates that the influence of temperature on the contact angle is reduced with the increase of suberic acid content.

3.4 Comparison with Young's equation

The Young's equation used to describe the contact angle of a droplet on a plate surface is given by

$$\cos\alpha' = \frac{\gamma_{sv} - \gamma_{sl}}{\gamma_{lv}} \quad (6)$$

where α', γ_{lv}, γ_{sv} and γ_{sl} are the contact angle, liquid-gas surface tension, solid-gas surface tension, and solid-liquid surface tension, respectively. However, in the LLPS droplets, the water (-NaCl) clusters approximately present as complete spheres, and dodecane adheres to the spherical water (-NaCl) clusters in the shape of spherical lenses, which wets the spherical water (-NaCl) clusters, partially. Therefore, spherical water (-

https://doi.org/10.5194/egusphere-2026-1577
Preprint. Discussion started: 11 May 2026

NaCl) clusters in LLPS droplets can be regarded as "plates", and the contact angle can be calculated by:

$$\cos\alpha = \frac{\gamma_{wv} - \gamma_{wo}}{\gamma_{ov}} \quad (7)$$

where γ_{wv}, γ_{ov} and γ_{wo} represent the water-gas, organic-gas, and water-organic surface tensions, respectively. This definition for the contact angle has been applied to study of LLPS contact angles (Qiu and Molinero, 2015).

To compare the predictions of Young's equation results with the MD simulation results, we quantitively analyzed gas-liquid interfacial tensions (NaCl solution, $\gamma_{g\text{-}w(NaCl)}$, pure dodecane, $\gamma_{g\text{-}d}$) and liquid-liquid interfacial tension (NaCl solution-dodecane, $\gamma_{w(NaCl)\text{-}d}$) in binary and ternary systems, and the corresponding results are shown in Fig. 8. In Fig. 8, MD simulation results based on the Martini force field and the OPLS-UA force field are included. Results based on experiments (Schmidt et al., 1966; Sayed et al., 2019; Seinfeld and Pandis, 2016) and MD simulations (Marrink et al., 2007; Ndao et al., 2015; Chen and Smith, 2007) in literatures are also included to validate MD simulations in this study.

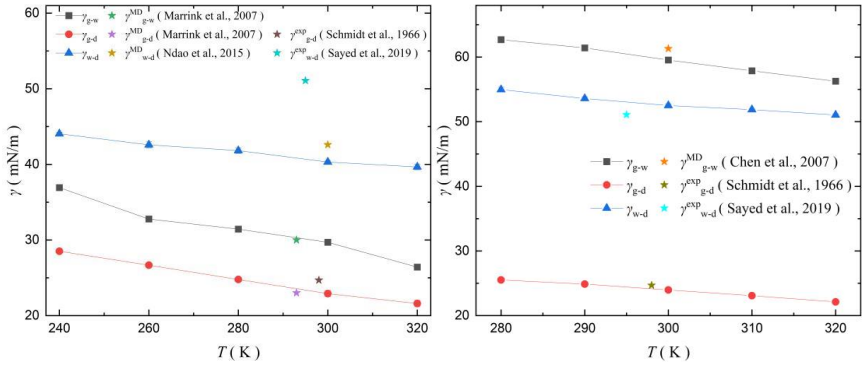

(a) (b)

https://doi.org/10.5194/egusphere-2026-1577
Preprint. Discussion started: 11 May 2026

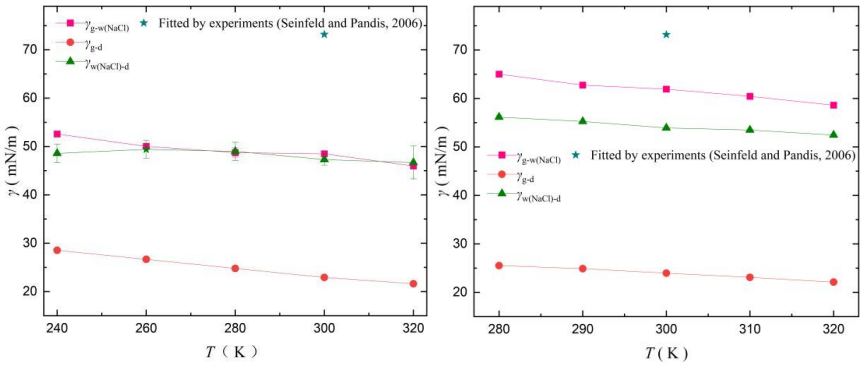

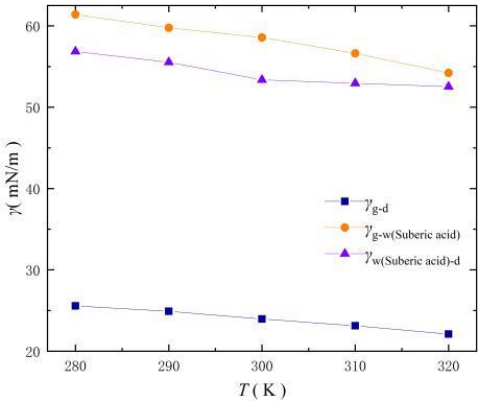

Fig. 8. Interfacial tensions of gas- NaCl solution/suberic acid solution ($\gamma_{g\text{-}w}$, $\gamma_{g\text{-}w(NaCl)}$, $\gamma_{g\text{-}w(suberic\ acid)}$), gas-pure dodecane $\gamma_{g\text{-}d}$, and NaCl solution/suberic acid solution-dodecane, ($\gamma_{w(NaCl)\text{-}d}$, $\gamma_{w(NaCl)\text{-}d}$, $\gamma_{w(suberic\ acid)\text{-}d}$), based on Martini force field (a, c) and OPLS-UA force field (b, d, e), existing results from experiments (Schmidt et al., 1966; Sayed et al., 2019; Seinfeld and Pandis, 2016) and MD simulations (Marrink et al., 2007; Ndao et al., 2015; Chen and Smith, 2007) are presented

For the binary water-dodecane system, it can be found from Fig. 8(a) that at T = 300 K, the gas-water interfacial tension obtained in this paper is 31 mN·m^{-1}, which is approximately consistent with the simulation results based on the Martini force field in

https://doi.org/10.5194/egusphere-2026-1577
Preprint. Discussion started: 11 May 2026

the literature (Marrink et al., 2007). For the gas-water interfacial tension, the divergence between the results of Martini force field MD simulation and the experiment (72.5 $mN \cdot m^{-1}$) has been reported in previous studies, which is considered as an inherent limitation of the Martini force field (Marrink et al., 2007). However, for the gas-dodecane interfacial tension, the simulation results in this paper are in good agreement with previous simulation results based on the Martini force field and experimental outcomes (Schmidt et al., 1966; Marrink et al., 2007). Furthermore, the interfacial tension between dodecane and water in this study is approximately consistent with the existing MD simulation results, and it is approximately 5 $mN \cdot m^{-1}$ smaller than the experimental results. Besides, Fig. 8(a) demonstrates that $\gamma_{g\text{-}w}$, $\gamma_{g\text{-}d}$ and $\gamma_{w\text{-}d}$ obtained from the Martini force field decrease with the increase of temperature. As shown in Fig. 8(b), $\gamma_{g\text{-}w}$ and $\gamma_{w\text{-}d}$ obtained based on the OPLS-UA force field are significantly greater than the results of the Martini force field and are closer to the experimental results (Ndao et al., 2015; Sayed et al., 2019). Furthermore, $\gamma_{g\text{-}w}$, $\gamma_{g\text{-}d}$ and $\gamma_{w\text{-}d}$ obtained based on the OPLS-UA force field also exhibit a negative correlation with the temperature.

For the ternary water-dodecane-NaCl system, Fig. 8(c) and 8(d) show that the $\gamma_{g\text{-}w(NaCl)}$ and $\gamma_{w(NaCl)\text{-}d}$ values obtained using the Martini force field are smaller than those based on the OPLS-UA force field. The $\gamma_{g\text{-}w(NaCl)}$ values derived from both force fields are lower than those from the experimental fitting formula. Furthermore, $\gamma_{g\text{-}w(NaCl)}$ and $\gamma_{w(NaCl)\text{-}d}$ based on both Martini force field and OPLS-UA force field exhibit a negative correlation with temperature. In Fig. 8(e), it can be observed that in the ternary water-dodecane-suberic acid system both $\gamma_{g\text{-}w(suberic\ acid)}$ and $\gamma_{w(suberic\ acid)\text{-}d}$ are negatively

https://doi.org/10.5194/egusphere-2026-1577
Preprint. Discussion started: 11 May 2026

correlated with the temperature, which is consistent with other interfacial tensions in Fig. 8.

Based on the interfacial tension from MD simulation, Young's equation (Equation (7)) can be used to calculate the liquid-liquid contact angle of the LLPS droplets. To assess the accuracy of the Young's equation in the prediction of the liquid-liquid contact angle, Fig. 9 presents the liquid-liquid contact angles of binary dodecane-water droplets and ternary water-dodecane-NaCl droplets obtained from direct MD simulation (using both the Martini force field and the OPLS-UA force field) and Young's equation.

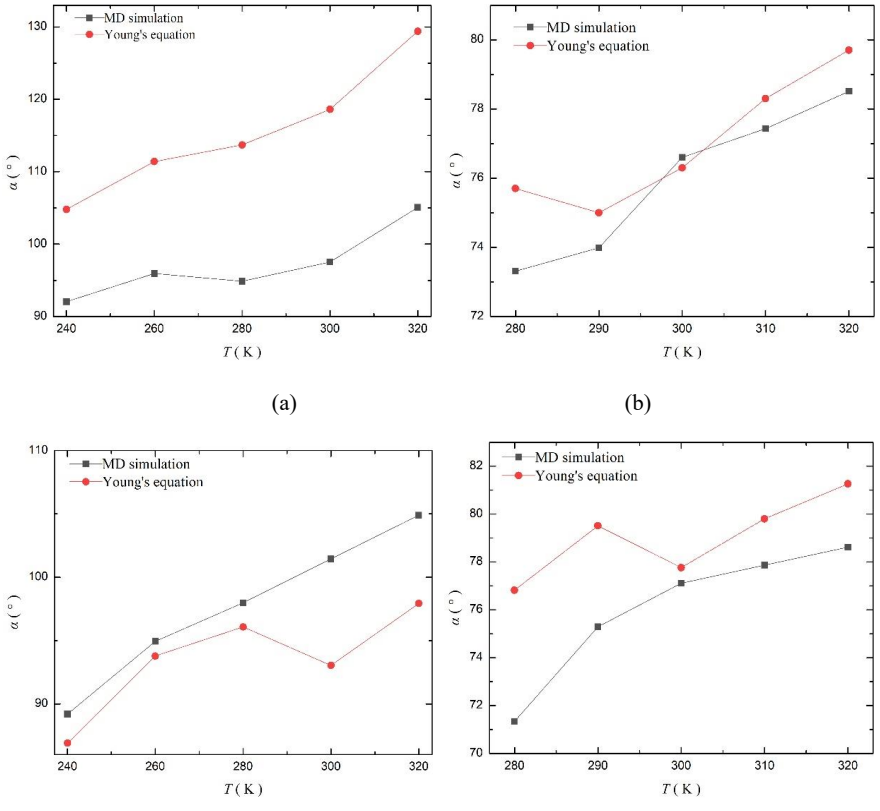

https://doi.org/10.5194/egusphere-2026-1577
Preprint. Discussion started: 11 May 2026

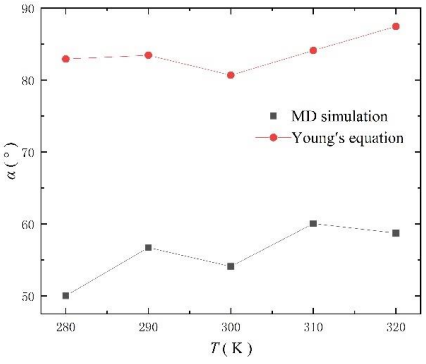

(e)

Fig. 9. Comparison of the contact angle results based on direct MD simulation (using both the Martini force field (a, c) and the OPLS-UA force field (b, d, e)) and Young's equation (Equation (7)), (a, b) for binary water-dodecane system, (c, d) for ternary water-dodecane-NaCl system and (e) for ternary water-dodecane-suberic acid system

It can be observed from Fig. 9(a) that in the binary water-dodecane droplets, the liquid-liquid contact angles obtained from Young's equation are significantly greater than those predicted by MD simulations using the Martini force field under various temperature conditions. Fig. 9(b) shows that there is also a discrepancy between the liquid-liquid contact angles derived from Young's equation and the MD simulation results based on the OPLS-UA force field, while this difference is smaller than that observed in Fig. 9(a). As shown in Fig. 9(c) and Fig. 9(d), for the ternary water-dodecane-NaCl droplets, the liquid-liquid contact angles obtained from Young's equation are notably lower than those predicted by the Martini force field MD simulations while higher than those predicted by the OPLS-UA force field MD simulations. For the ternary water-dodecane-suberic acid system (Fig. 9(e)), the liquid-liquid contact angles calculated by Young's equation are larger than the MD simulation

https://doi.org/10.5194/egusphere-2026-1577
Preprint. Discussion started: 11 May 2026

results based on the OPLS-UA force field. All droplet diameters in our MD simulations are less than 20 nm, so it can be inferred that Young's equation deviates significantly from the simulated contact angles for the nanoscale droplets examined in this study, which is consistent with previous studies on liquid-solid contact angle and liquid-liquid contact angle in the nanoscale (Qiu and Molinero, 2015; Jabbarzadeh, 2024).

In the nanoscale, Qiu and Molinero (2015) derived a modified version of the Young's equation by introducing linear tension into the calculation of the free energy of the droplet structure.

$$\gamma_{wo} - \gamma_{wv} + \gamma_{ov} \times \cos\alpha + \frac{r_w - r_o \times \cos\alpha}{r_w \times r_o \times \sin\alpha}\tau = 0 \quad (8)$$

where τ represents the linear tension, indicating the excess energy per unit length of the three-phase contact line among two liquid phases and the gas phase. This formula has also been derived in the study of liquid nucleation on curved surfaces (Iwamatsu, 2015). Qiu and Molinero (2015) calculated the contact angle between nonane and water based on MD simulations, yielding a line tension range from -20×10^{-12} N to 5×10^{-12} N.

Fig. 10 presents the line tension calculated based on Equation (8) and MD simulations with both Martini force field and the OPLS-UA force field, and results for water-dodecane system, water-dodecane-NaCl and water-dodecane-suberic acid systems are included.

As shown in Fig. 10(a) and Fig. 10(b), the line tensions for binary water-dodecane systems based on the Martini force field vary from -4.56×10^{-11} N to -3.33×10^{-11} N, and results based on the OPLS-UA force field range from -9.82×10^{-12} N to 1.03×10^{-12} N. These results are comparable in magnitude to the reported value of $\tau = 1.69 \pm 0.3\times10^{-11}$

https://doi.org/10.5194/egusphere-2026-1577
Preprint. Discussion started: 11 May 2026

N for dodecane on a horizontal surface (Aveyard et al., 1999). For ternary water-dodecane-NaCl systems (Fig. 10(c) and Fig. 10(d)), it can be observed that the line tensions based on the Martini force field and the OPLS-UA force field are 2.64×10^{-12} N~14.23×10^{-12} N, and -25.3×10^{-12} N~2.26×10^{-12} N, respectively. For ternary water-dodecane-suberic acid systems, Fig. 10(e) shows that the line tensions based on the OPLS-UA force field range from -1.72×10^{-9} N to -1.8×10^{-11} N. Line tensions presented in Fig. 10 can be fitted into a fourth-order polynomial function of temperature (equation (9)), and the parameters are listed in Table S8.

$$\tau = a1 + a2 \times T + a3 \times T^2 + a4 \times T^3 + a5 \times T^4 \quad (9)$$

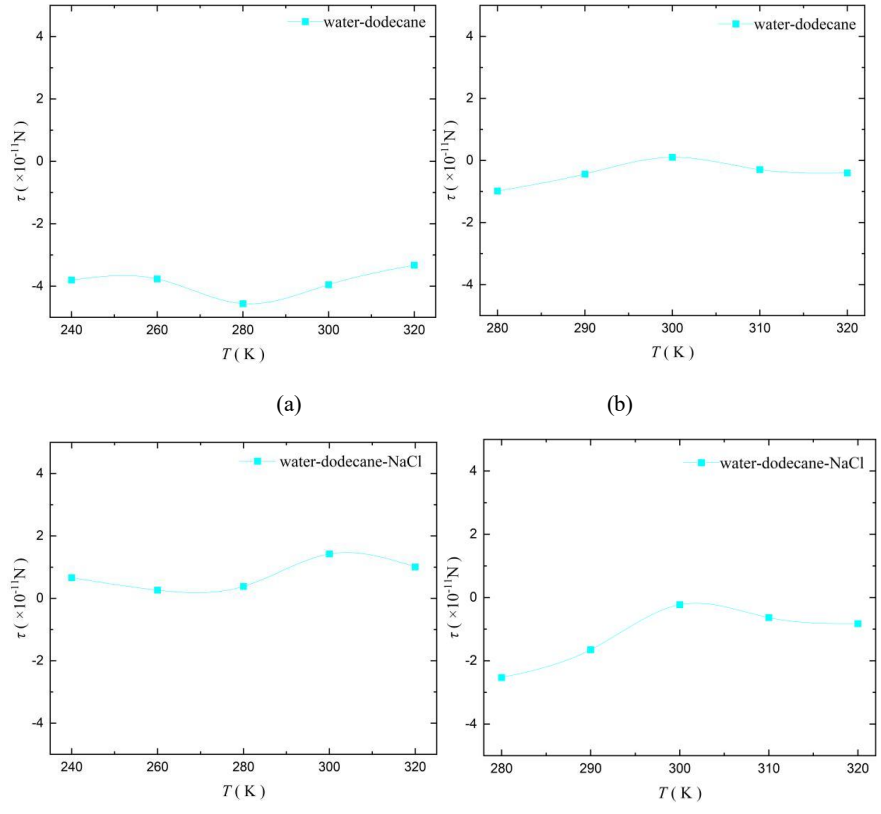

https://doi.org/10.5194/egusphere-2026-1577
Preprint. Discussion started: 11 May 2026

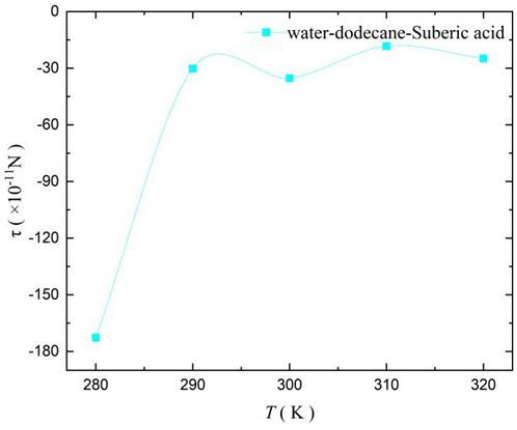

(e)

Fig. 10. The line tensions calculated using Equation (8) and MD simulations with both Martini force field (a, c) and OPLS-UA force field (b, d, e), (a, b) for binary water-dodecane system, (c, d) for ternary water-dodecane-NaCl systems and (e) for ternary water-dodecane-suberic acid system

3.5 Discussions

For all LLPS particles studied in this work, the contact angle is positively correlated with the temperature, which is different from the results for contact angle of water droplets on a horizontal surface. For hydrophilic horizontal surface, the contact angle of water droplet has been found to decrease with the increasing temperature (Villa et al., 2018). It can be explained based on the Young's equation (Equation (6)), that is, the increasing temperature leads to a decrease in γ_{lv} and γ_{sl}, resulting in a decrease in contact angle. For smooth hydrophobic horizontal surface, as the temperature increases, no significant change in the contact angle can be observed (Villa et al., 2018; Heydari et al., 2013). As the temperature increases, the decreasing γ_{lv} leads to an increase in the contact angle because the cosine value of the contact angle is negative. However, the

https://doi.org/10.5194/egusphere-2026-1577
Preprint. Discussion started: 11 May 2026

increase of γ_{sv} - γ_{sl} (negative value) results in a decrease in the contact angle, which will offset the effect of the decreasing γ_{lv}. For the superhydrophobic surface, when the temperature is higher than the dew point, the contact angle is almost unaffected by temperature changes. It is because that the water droplet sits on a trapped air cushion (Cassie-Baxter state), which minimizes direct contact and reduces the influence of surface temperature on interfacial tensions at the contact line. However, when the temperature drops below the dew point, the contact angle decreases significantly with the decrease in temperature, which can be explained by that the water vapor condensation fills the air pockets within the surface microstructure, causing a transition from the Cassie-Baxter state (air-cushioned) to the Wenzel state (fully wetted) (Marmur, 2003).

The traditional Young's equation (Equation (6)) can also be adopted to explain the correlation between temperature and contact angle in LLPS particle obtained by MD simulations, because they have consistent qualitative results. Therefore, for LLPS particle, the positive correlation between temperature and contact angle may be because the decrease in γ_{wv}-γ_{ov} is greater than the decrease in γ_{wo} with the increase of temperature.

Results of MD simulation in this study show that the liquid-liquid contact angle of the water-dodecane-NaCl system decreases with increasing NaCl concentration (Fig. 5), and the contact angle of the water-dodecane-suberic acid system decreases with increasing sebacic acid concentration (Fig. 7). These can also be explained by Equation (6). In the water-dodecane-NaCl system, the increase in NaCl concentration results in an increase in interfacial tension between the gas and the NaCl solution (Seinfeld and

https://doi.org/10.5194/egusphere-2026-1577
Preprint. Discussion started: 11 May 2026

Pandis, 2016), while the salting-out effect of NaCl will increase the interfacial tension between the NaCl solution and dodecane (Remesal et al., 2017). The former increases to a greater extent than the latter, resulting in a decrease in contact angle. In the water-dodecane-suberic acid system, the increase in suberic acid concentration leads to a decrease in both gas-liquid (suberic acid solution) interfacial tension and liquid (suberic acid solution)-liquid (dodecane) interfacial tension. However, the decrease in the former is less pronounced than that in the latter, resulting in a reduction in the liquid-liquid contact angle.

The contact angle in LLPS aerosol particle has a significant impact on the hygroscopicity and CCN activities in equilibrium state and the condensation and evaporation rate in the non-equilibrium state. In the Köhler theory (Köhler, 1936), surface tension is a key parameter in the Kelvin term, and in some literatures the effective surface tension of the droplet was calculated as the surface-area-weighted mean of the composition-dependent surface tensions from both phases (Ovadnevaite et al., 2017; Huang et al., 2021). Including the contact angle between liquid and liquid phases is able to make the calculation of surface tension more accurate. The heat and mass accommodation coefficients are key parameters in the theoretical model of heat and mass transfer at gas-liquid interface (Zhang et al., 2025; Shiraiwa et al., 2010; Nguyen et al., 2026), but they cannot be measured directly. In many existing studies, heat and mass accommodation coefficients are always set to 1 or a fixed empirical value, which may be unreasonable.

If the adsorption coefficient of each liquid phase in the liquid-liquid phase

https://doi.org/10.5194/egusphere-2026-1577
Preprint. Discussion started: 11 May 2026

separation particles is known, the equivalent accommodation coefficients can be obtained based on the surface-area-weighted mean which can be calculated by the contact angle. In addition, the contact angle is able to affect the mass transfer between two liquid phases by affecting the contact area between two liquid phases. This study provides ideas for the quantitative description of contact angle, and in the future, the calculation method of contact angle can be improved through the study of LLPS particles with various components and sizes.

4 Conclusions

This study employs MD simulations with the Martini and OPLS-UA force fields to quantify the liquid-liquid contact angle of LLPS water-dodecane aerosols. It aims to elucidate the effects of temperature, water content, NaCl and suberic acid, and further assess the applicability of Young's equation at the nanoscale. Results shows that in binary water-dodecane LLPS particles the contact angle increases with temperature and water content. In the ternary water-dodecane-NaCl LLPS particles the contact angle is negatively correlated with the NaCl concentration but positively correlated with temperature, and the Martini force field yields larger contact angles and stronger NaCl-induced reduction above 200 ion pairs due to the formation of the ellipsoidal structure. In the ternary water-dodecane-suberic acid LLPS particles the contact angle is negatively correlated with the suberic acid content but positively correlated with temperature, and the effect of temperature on the contact angle decreases with the increase of the suberic acid content. The OPLS-UA force field yields gas-water and water-dodecane interfacial tensions in better agreement with experimental data than the

https://doi.org/10.5194/egusphere-2026-1577
Preprint. Discussion started: 11 May 2026

Martini force field. The contact angle based on the classical Young's equation deviates noticeably from nanoscale MD results. This discrepancy can be eliminated by the line tension correction, and the fitted line tension is well described by a fourth-order polynomial of temperature. Results agree with Qiu and Molinero (2015) on the "Russian doll" morphology and nanoscale line tension effects, and with Jabbarzadeh (2024) on the breakdown of classical Young's equation at the nanoscale. This work extends prior studies by quantifying combining effects of NaCl, surfactant and temperature on the liquid-liquid contact angle and comparing two force fields systematically. The positive temperature-contact angle relationship differs from macroscale liquid-solid wetting, highlighting unique behavior in LLPS aerosol systems. The effects of NaCl and suberic acid on the contact angle is due to their influences on different interfacial tensions.

The model systems are simplified relative to real atmospheric aerosols containing multiple organics and salts, and results apply to droplets smaller than 20 nm and cannot be directly extrapolated to larger sizes. Future work should examine multicomponent mixtures and broader size ranges. At the atmospheric scale, the liquid–liquid contact angle governs the morphology, hygroscopic growth and CCN activity of LLPS aerosols. Incorporating accurate contact angle values improves surface tension calculations in Köhler theory, and further refines the mass/heat accommodation coefficients as well as liquid–liquid contact area estimations in heat and mass transfer theory. These findings advance the thermodynamic representation of LLPS aerosols, supporting more reliable projections of aerosol–cloud interactions, radiative forcing, and climate change.

https://doi.org/10.5194/egusphere-2026-1577
Preprint. Discussion started: 11 May 2026

Code and data availability.

The data that support the findings of this study are available from the corresponding author upon reasonable request.

Supplement.

The supplement related to this article is available online.

Author contributions.

CZ conceptualized the study, designed the research, and wrote the manuscript. **LYL, SPL and HYL** performed the formal analysis and data validation. **NM** contributed to the writing of introduction and discussion sections, and revised the initial draft. **YY**, **YSW and AW** supervised the project, and provided guidance on data quality control. All authors participated in discussing the results and editing the manuscript, and approved the final version for submission.

Competing interests

The contact author has declared that none of the authors has any competing interests.

Acknowledgments

The authors are grateful to the support from the National Natural Science Foundation of China (Nos. 52576167, 52106207, 42530602). We would also like to thank the financial support from State Administration of Foreign Experts Affairs (China)

https://doi.org/10.5194/egusphere-2026-1577
Preprint. Discussion started: 11 May 2026

(H20250966, G2022013042L) and Science and Technology Commission of Shanghai Municipality (STCSM) (22WZ2502600).

References

Aveyard, R., Clint, J. H., Nees, D., and Paunov, V.: Size-dependent lens angles for small oil lenses on water, Colloids and Surfaces A: Physicochemical and Engineering Aspects, 146, 95-111, 1999.

Bahadur, R. and Russell, L. M.: Effect of surface tension from MD simulations on size-dependent deliquescence of NaCl nanoparticles, Aerosol Sci. Technol., 42, 369-376, 2008.

Blokhuis, E., Bedeaux, D., Holcomb, C., and Zollweg, J.: Tail corrections to the surface tension of a Lennard-Jones liquid-vapour interface, Mol. Phys., 85, 665-669, 1995.

Chen, F. and Smith, P. E.: Simulated surface tensions of common water models, J. Chem. Phys., 126, 2007.

Davies, J. F.: Mass, charge, and radius of droplets in a linear quadrupole electrodynamic balance, Aerosol Science Technology, 53, 309-320, 2019.

Do Hong, S., Ha, M. Y., and Balachandar, S.: Static and dynamic contact angles of water droplet on a solid surface using molecular dynamics simulation, Journal of colloid and interface science, 339, 187-195, 2009.

Freedman, M. A.: Phase separation in organic aerosol, Chemical Society Reviews, 46, 7694-7705, 2017.

Heydari, G., Thormann, E., Jarn, M., Tyrode, E., and Claesson, P. M. J. T. J. o. P. C. C.:

https://doi.org/10.5194/egusphere-2026-1577
Preprint. Discussion started: 11 May 2026

608 Hydrophobic surfaces: topography effects on wetting by supercooled water and
609 freezing delay, 117, 21752-21762, 2013.
610 Huang, Y., Mahrt, F., Xu, S., Shiraiwa, M., and Bertram, A. K.: Coexistence of three
611 liquid phases in individual atmospheric aerosol particles, Proc. Natl. Acad. Sci. U.S.A.,
612 118, e2102512118, 2021.
613 Ingram, S., Rovelli, G., Song, Y.-C., Topping, D., Dutcher, C. S., Liu, S., Nandy, L.,
614 Shiraiwa, M., and Reid, J. P.: Accurate prediction of organic aerosol evaporation using
615 kinetic multilayer modeling and the Stokes–Einstein Equation, J. Phys. Chem. A, 125,
616 3444-3456, 2021.
617 Iwamatsu, M.: Line-tension effects on heterogeneous nucleation on a spherical
618 substrate and in a spherical cavity, Langmuir, 31, 3861-3868, 2015.
619 Jabbarzadeh, A.: Effect of molecular branching and surface wettability on solid-liquid
620 surface tension and line-tension of liquid alkane surface nanodroplets, Journal of
621 Colloid Interface Science, 666, 355-370, 2024.
622 Jorgensen, W. L., Madura, J. D., and Swenson, C. J.: Optimized intermolecular potential
623 functions for liquid hydrocarbons, J. Am. Chem. Soc., 106, 6638-6646, 1984.
624 Karadima, K. S., Mavrantzas, V. G., and Pandis, S. N.: Insights into the morphology of
625 multicomponent organic and inorganic aerosols from molecular dynamics simulations,
626 Atmos. Chem. Phys., 19, 5571-5587, 2019.
627 Köhler, H.: The nucleus in and the growth of hygroscopic droplets, Trans. Faraday Soc.,
628 32, 1152-1161, 1936.
629 Leong, K.-Y. and Wang, F.: A molecular dynamics investigation of the surface tension

https://doi.org/10.5194/egusphere-2026-1577
Preprint. Discussion started: 11 May 2026

of water nanodroplets and a new technique for local pressure determination through density correlation, J. Chem. Phys., 148, 2018.

Marmur, A.: Wetting on hydrophobic rough surfaces: to be heterogeneous or not to be?, Langmuir, 19, 8343-8348, 2003.

Marrink, S. J., Risselada, H. J., Yefimov, S., Tieleman, D. P., and De Vries, A. H.: The MARTINI force field: coarse grained model for biomolecular simulations, J. Phys. Chem. B, 111, 7812-7824, 2007.

Martin, S. T.: Phase transitions of aqueous atmospheric particles, Chemical Reviews, 100, 3403-3454, 2000.

Ndao, M., Devémy, J., Ghoufi, A., and Malfreyt, P.: Coarse-graining the liquid–liquid interfaces with the MARTINI force field: How is the interfacial tension reproduced?, Journal of Chemical Theory Computation, 11, 3818-3828, 2015.

Nguyen, K., Schervish, M., Lakey, P. S., Smith, J. N., and Shiraiwa, M.: Impact of particle phase state on the competition between condensation and coagulation, Environmental Science: Atmospheres, 2026.

Noziere, B., Baduel, C., and Jaffrezo, J.: The dynamic surface tension of atmospheric aerosol surfactants reveals new aspects of cloud activation, Nat. Commun., 5, 3335-3335, 2014.

O'Brien, R. E., Wang, B., Kelly, S. T., Lundt, N., You, Y., Bertram, A. K., Leone, S. R., Laskin, A., and Gilles, M. K.: Liquid–liquid phase separation in aerosol particles: Imaging at the nanometer scale, Environ. Sci. Technol., 49, 4995-5002, 2015.

Obeidat, A., Hrahsheh, F., and Wilemski, G.: Scattering Form Factors for Russian Doll

https://doi.org/10.5194/egusphere-2026-1577
Preprint. Discussion started: 11 May 2026

652 Aerosol Droplet Models, J. Phys. Chem. B, 119, 9304-9311, 2015.

653 Ovadnevaite, J., Zuend, A., Laaksonen, A., Sanchez, K. J., Roberts, G., Ceburnis, D.,
654 Decesari, S., Rinaldi, M., Hodas, N., and Facchini, M. C.: Surface tension prevails over
655 solute effect in organic-influenced cloud droplet activation, Nature, 546, 637-641, 2017.

656 Papon, P., Leblond, J., and Meijer, P. H.: Dynamics of Phase Transitions, in: The
657 Physics of Phase Transitions: Concepts and Applications, Springer, 37-78, 2006.

658 Qiu, Y. and Molinero, V.: Morphology of liquid–liquid phase separated aerosols, J. Am.
659 Chem. Soc., 137, 10642-10651, 2015.

660 Rehner, P., Aasen, A., and Wilhelmsen, Ø.: Tolman lengths and rigidity constants from
661 free-energy functionals—General expressions and comparison of theories, J. Chem.
662 Phys., 151, 2019.

663 Remesal, E. R., Suárez, J. A., Márquez, A. M., Sanz, J. F., Rincón, C., and Guitián, J.:
664 Molecular dynamics simulations of the role of salinity and temperature on the
665 hydrocarbon/water interfacial tension, Theoretical Chemistry Accounts, 136, 66, 2017.

666 Sayed, A. M., Olesen, K. B., Alkahala, A. S., Sølling, T. I., and Alyafei, N.: The effect
667 of organic acids and salinity on the interfacial tension of n-decane/water systems,
668 Journal of Petroleum Science Engineering, 173, 1047-1052, 2019.

669 Schmedding, R. and Zuend, A.: The role of interfacial tension in the size-dependent
670 phase separation of atmospheric aerosol particles, Atmos. Chem. Phys., 25, 327-346,
671 2025.

672 Schmidt, R. L., Randall, J. C., and Clever, H. L.: The surface tension and density of
673 binary hydrocarbon mixtures: benzene-n-hexane and benzene-n-dodecane, The Journal

https://doi.org/10.5194/egusphere-2026-1577
Preprint. Discussion started: 11 May 2026

of Physical Chemistry, 70, 3912-3916, 1966.

Seinfeld, J. H. and Pandis, S. N.: Atmospheric chemistry and physics: from air pollution to climate change, John Wiley & Sons2016.

Sergi, D., Scocchi, G., and Ortona, A.: Coarse-graining MARTINI model for molecular-dynamics simulations of the wetting properties of graphitic surfaces with non-ionic, long-chain, and T-shaped surfactants, J. Chem. Phys., 137, 2012.

Shiraiwa, M., Pfrang, C., Pöschl, U. J. A. C., and Physics: Kinetic multi-layer model of aerosol surface and bulk chemistry (KM-SUB): the influence of interfacial transport and bulk diffusion on the oxidation of oleic acid by ozone, 10, 3673-3691, 2010.

Shiraiwa, M., Zuend, A., Bertram, A. K., and Seinfeld, J. H.: Gas–particle partitioning of atmospheric aerosols: interplay of physical state, non-ideal mixing and morphology, Phys. Chem. Chem. Phys., 15, 2013.

Song, M., Marcolli, C., Krieger, U., Zuend, A., and Peter, T.: Liquid-liquid phase separation and morphology of internally mixed dicarboxylic acids/ammonium sulfate/water particles, Atmos. Chem. Phys., 12, 2691-2712, 2012.

Tang, I. and Munkelwitz, H.: Aerosol phase transformation and growth in the atmosphere, Journal of Applied Meteorology, 791-796, 1994.

Tolman, R. C.: The effect of droplet size on surface tension, J. Chem. Phys., 17, 333-337, 1949.

Veghte, D. P., Altaf, M. B., and Freedman, M. A.: Size dependence of the structure of organic aerosol, J. Am. Chem. Soc., 135, 16046-16049, 2013.

Villa, F., Marengo, M., and De Coninck, J. J. S. r.: A new model to predict the influence

https://doi.org/10.5194/egusphere-2026-1577
Preprint. Discussion started: 11 May 2026

of surface temperature on contact angle, 8, 6549, 2018.

You, Y., Renbaum-Wolff, L., Carreras-Sospedra, M., Hanna, S. J., Hiranuma, N., Kamal, S., Smith, M. L., Zhang, X., Weber, R. J., and Shilling, J. E.: Images reveal that atmospheric particles can undergo liquid–liquid phase separations, Proc. Natl. Acad. Sci. U.S.A., 109, 13188-13193, 2012.

Young, T.: III. An essay on the cohesion of fluids, Philosophical Transactions of the Royal Society of London. Series A, Containing Papers of a Mathematical or Physical Character, 65-87, 1805.

Yu, H., Kaufman, Y., Chin, M., Feingold, G., Remer, L., Anderson, T., Balkanski, Y., Bellouin, N., Boucher, O., and Christopher, S.: A review of measurement-based assessments of the aerosol direct radiative effect and forcing, Atmos. Chem. Phys., 6, 613-666, 2006.

Zhang, C., Zhang, Z., Xiong, W., Yang, Y., and Wang, Y.: Molecular dynamics investigation on structural and interfacial characteristics of aerosol particles containing mixed organic components, Atmos. Environ., 319, 120305, 2024.

Zhang, C., Lu, M., Bao, H., Ma, N., Yu, D., Yang, Y., Wang, Y., and Wiedensohler, A.: An improved model on the evaporation kinetics of the single aerosol droplet and its application for the droplet composed of ammonium sulfate or sucrose solution, Powder Technol., 120627, 2025.

Zuend, A., Marcolli, C., Luo, B. P., and Peter, T.: A thermodynamic model of mixed organic-inorganic aerosols to predict activity coefficients, Atmos. Chem. Phys., 8, 4559-4593, 2008.

https://doi.org/10.5194/egusphere-2026-1577
Preprint. Discussion started: 11 May 2026

718 Zuend, A., Marcolli, C., Peter, T., and Seinfeld, J. H.: Computation of liquid-liquid
719 equilibria and phase stabilities: implications for RH-dependent gas/particle partitioning
720 of organic-inorganic aerosols, Atmos. Chem. Phys., 10, 7795-7820, 2010.
721